Available online at www.sciencedirect.com

ScienceDirect

Procedia CIRP 53 (2016) 237 – 246

www.elsevier.com/locate/procedia

The 10th International Conference on Axiomatic Design, ICAD 2016

Axiomatic design method for supercritical rotor dynamics integrating nonlinear deep knowledge

Yingze Jin, Zhaoyang Shi, Honglun Hong, Fan Zhang, Xiaoyang Yuan*

Key Laboratory of Education Ministry for Modern Design and Rotor-Bearing System, Xi'an Jiaotong University, Xi'an 710049, China

* Corresponding author. Tel.: +86-029-82669152; fax: +86-18642736066. *E-mail address:* jinyingze@stu.xjtu.edu.cn

Abstract

This paper integrates nonlinear deep knowledge with an axiomatic design method for supercritical rotor dynamics in order to overcome the limitation of rotor dynamic design for supercritical rotating machineries. Design methods based on linear theory usually lead to shafting failures in engineering practice, since nonlinear theory has not been well incorporated into rotor dynamic design. This method realizes a four-level decomposition of the functional requirements and mapping of the corresponding design parameters in nonlinear dynamic design for a supercritical rotor-bearing system. In total, 20 design parameters are integrated into the system. A 20×20 axiomatic design matrix is then developed, which is used to obtain a dynamic design flowchart of the system. Under the guidance of the design flowchart, a single span flexible symmetric rotor-bearing system with a single disk is dynamically designed and analyzed. The results show that the axiomatic design method for supercritical rotor dynamics optimizes the design process, the design efficiency and the design results.

Peer-review under responsibility of the scientific committee of The 10th International Conference on Axiomatic Design

Keywords: Axiomatic design method; Nonlinear deep knowledge; Supercritical rotor dynamics

1. Introduction

Due to the effect of nonlinear oil-film forces on journal bearings, rotor-bearing systems are strongly nonlinear dynamic systems. Linear theory of rotor-bearing systems has already been developed and has been widely applied to rotor dynamic design. Linear theory is simple and easy to understand, and it can accurately reflect the objective laws of system vibration in most cases when the amplitude is small enough. Therefore, current rotor dynamic design methods are still based on linear theory, and nonlinear theory is mainly used for particular types of handling after failure of rotating machineries. However, rotating machineries are now being developed for high speed operation in supercritical rotating machinery applications such as turbines, compressors and pumps. These rotors all have working speeds that are far higher than the first critical speeds and thus will produce strong self-excited vibrations, leading to system instabilities and even generating complicated nonlinear phenomena such as bifurcations, chaos and subharmonic resonances. Therefore, it is extremely inappropriate to adopt linear theory for the dynamic design of these systems, as it usually leads to shafting failures in engineering practice. Fortunately, there is currently a lot of research into rotor-bearing systems based on nonlinear theory, and a number of achievements have been made, particularly in relation to the nonlinear dynamic behavior and stability analysis of these systems [1,2]. However, nonlinear deep knowledge is complicated and difficult to understand, and has not yet been adequately incorporated into rotor dynamic design. It is hard to manage the fact that introduction of nonlinear deep knowledge increases the complexity of rotor dynamic design in comparison with general design theories. Since axiomatic design theory has distinct advantages for handling complicated design propositions, this paper builds a design method for supercritical rotor dynamics based on axiomatic design theory.

Axiomatic design theory was first proposed by Suh, a professor at Massachusetts Institute of Technology. It is a scientific design methodology which can be applied to a wide range of fields and is based on logical and rational thinking [3,4]. The theory has shown good applicability in the design

Peer-review under responsibility of the scientific committee of The 10th International Conference on Axiomatic Design
doi:10.1016/j.procir.2016.06.100

of complex systems and dynamics [5-10]. In order to introduce nonlinear theory of rotor-bearing systems into rotor dynamic design and integrate nonlinear deep knowledge research, an axiomatic design method for supercritical rotor dynamics is adopted. In contrast with prevalent rotor dynamic designs which are based on linear theory, this method can genuinely reflect the critical speeds, threshold speeds and various complex nonlinear phenomena that may appear in rotor-bearing systems under actual working conditions, and provides reference value that can be used by designers to select optimal design schemes. Taking axiomatic design theory as a guide and nonlinear theory as a basis, the paper realizes nonlinear dynamic design for supercritical rotor-bearing systems. The main works of this paper are organized as follows: i) The four domains of the design world and the two axioms of axiomatic design theory (the independence axiom and the information axiom) are introduced. ii) The independence axiom is adopted to realize nonlinear dynamic design for a supercritical rotor-bearing system. A four-level decomposition of the functional requirements and mapping of the corresponding design parameters are achieved within this design. A 20×20 axiomatic design matrix is developed, which is used to obtain a dynamic design flowchart of the system. iii) Under the guidance of this design flowchart, a single span flexible symmetric rotor-bearing system with a single disk is dynamically designed and analyzed. iv) The calculation results of the design example and the design results of the critical speed and threshold speed based on linear and nonlinear theories are discussed.

2. Key concepts of axiomatic design theory

The axiomatic design world is composed of four domains: the customer domain, the functional domain, the physical domain and the process domain. A structural diagram of the domains is shown in Fig.1. The domain on the left represents what we are trying to achieve, while the domain on the right represents how we want to achieve it.

In order to analyze and evaluate a design activity, axiomatic design theory provides two basic axioms — the independence axiom and the information axiom.

The first axiom, known as the independence axiom, requires that a design result must be able to meet each of the functional requirements (FRs) without affecting any of the other requirements when there are two or more FRs. This means that a set of correct design parameters (DPs) must be chosen to meet the FRs and maintain their independence. For a given design level, the functional requirement (FR) set that determines the specific design objectives forms a FR vector in the functional domain. Similarly, the design parameter (DP) set that has been selected to meet the FRs forms a DP vector in the physical domain. The relationship between the two vectors can be written using the following equation:

$$\{\mathrm{FR}\} = [A]\{\mathrm{DP}\} \tag{1}$$

where [*A*] is the design matrix and Formula (1) is the design equation.

In order to meet the independence axiom, the design matrix must be a diagonal matrix or a triangular matrix. When [*A*] is a diagonal matrix, each FR can be satisfied by one DP and the design is an uncoupled design. When [*A*] is a triangular matrix, if, and only if, the DPs are determined in a proper sequence, the independence of the FRs can be guaranteed and the design is a decoupled design. Any other forms of design matrices will lead to a coupled design. When there are three FRs and DPs, one type of [*A*] in the decoupled design can be expressed as:

$$[A] = \begin{bmatrix} X & 0 & 0 \\ 0 & X & 0 \\ X & X & X \end{bmatrix} \tag{2}$$

where *X* indicates that there is a coupling relationship between the FRs and the DPs and 0 means that there is no coupling relationship between the FRs and the DPs.

The design is a mapping process from the functional domain to the physical domain at the highest level. To complete the overall design activity, the FRs and the DPs at the highest level need to be decomposed and iterated at each level until the design can be enforced. The concrete process of decomposition and iteration is shown in Fig.2. The final decomposition result is represented by the green frames.

The second axiom, known as the information axiom, requires that the design possessing the minimum amount of information is the best design of all the designs that meet the independence axiom. The information content I_i of FR_i is defined by the success probability P_i of satisfying FR_i.

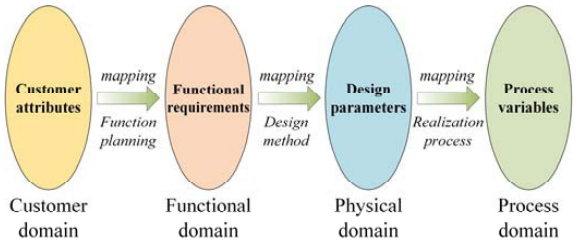

Fig. 1. The four domains of the axiomatic design world.

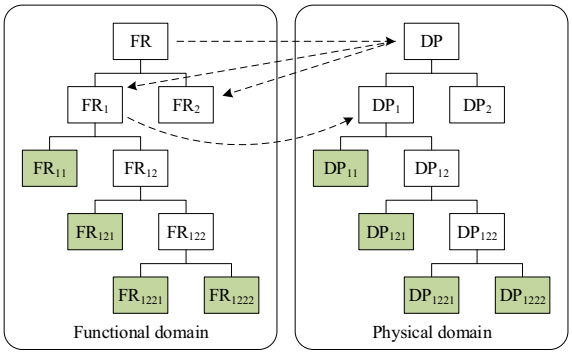

Fig. 2. The process of decomposition and iteration between the functional domain and the physical domain.

$$I_i = \log_2 \frac{1}{P_i} = -\log_2 P_i \tag{3}$$

In the actual design, the success probability is determined by the intersection between the design range stipulated by the designers and the system range offered by designers to satisfy the FR. Fig.3 shows the probability density function of a system within a system range that satisfies FR_i. The overlap between the design range and the system range is called the common range, and it is the only area that satisfies FR_i.

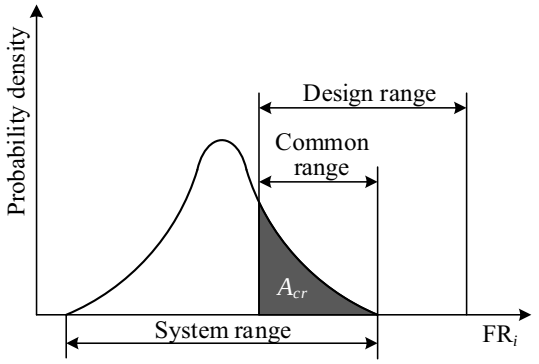

Fig. 3. The probability density function of a system within a system range that satisfies FR_i.

The success probability P_i of satisfying FR_i can be written as:

$$P_i = \int_a^b f\left(\mathrm{FR}_i\right)\mathrm{dFR}_i = A_{cr} \tag{4}$$

where f (FR_i) is the probability density function of the system satisfying FR_i, a is the lower limit of the design range, b is the upper limit of the design range, and A_{cr} is the area of the common range (the dark area in Fig.3).

3. Axiomatic design method for supercritical rotor dynamics

The first axiom of axiomatic design theory, the independence axiom, has been adopted to realize nonlinear dynamic design of a supercritical rotor system. Nonlinear dynamic design of the supercritical rotor-bearing system has been realized in order to calculate the stability, the critical speed and the unbalanced response of the system [1].

3.1. Decomposition of FRs and mapping of corresponding DPs at the first level

To achieve the supercritical rotor dynamic design, the rotor-bearing system vibration has firstly been calculated and the characteristics of the system have then been extracted so that designers can easily observe and analyze the vibration. A reasonable design scheme has finally been selected by designing the performance of the system under different parameter conditions. To finally obtain the overall FRs, the FRs at the first level can be decomposed as follows:

- FR_1: Calculate the vibration of the rotor-bearing system
- FR_2: Extract the characteristics of the rotor-bearing system
- FR_3: Design the performance of the rotor-bearing system

In order to meet these three FRs, three DPs can be chosen as follows:

- DP_1: The mathematical models of the rotor-bearing system
- DP_2: The graphs that reflect the characteristics of the rotor-bearing system
- DP_3: The graphs that reflect the nonlinear performance laws of the rotor-bearing system under different parameter conditions

The design equation of the first level can be written as:

$$\begin{Bmatrix} \mathrm{FR}_1 \\ \mathrm{FR}_2 \\ \mathrm{FR}_3 \end{Bmatrix} = \begin{bmatrix} X & 0 & 0 \\ X & X & 0 \\ X & X & X \end{bmatrix} \begin{Bmatrix} \mathrm{DP}_1 \\ \mathrm{DP}_2 \\ \mathrm{DP}_3 \end{Bmatrix} \tag{5}$$

The design matrix is a lower triangular matrix, which illustrates that the first level design is a decoupled design and satisfies the independence axiom.

3.2. Decomposition of FRs and mapping of corresponding DPs at the second level

For DP_1, the dynamic oil-film forces on the journal bearings and the kinetic equations of the rotor vibration need to be calculated. FR_1 can be decomposed as follows:

- FR_{11}: Calculate the dynamic oil-film forces on the journal bearings
- FR_{12}: Calculate the rotor vibration

In order to meet these two FRs, two DPs can be stipulated as follows:

- DP_{11}: The mathematical model based on Reynolds equation
- DP_{12}: The finite element model of the rotor

The design equation can be written as:

$$\begin{Bmatrix} \mathrm{FR}_{11} \\ \mathrm{FR}_{12} \end{Bmatrix} = \begin{bmatrix} X & 0 \\ X & X \end{bmatrix} \begin{Bmatrix} \mathrm{DP}_{11} \\ \mathrm{DP}_{12} \end{Bmatrix} \tag{6}$$

The design matrix is a lower triangular matrix, which illustrates that this is a decoupled design.

For DP_2, the time domain waveform, frequency spectrogram, axes track chart and Poincare mapping diagram of the rotor-bearing system need to be calculated. FR_2 can be decomposed as follows:

- FR_{21}: Calculate the time domain waveform of the rotor-bearing system
- FR_{22}: Calculate the frequency spectrum of the rotor-bearing system
- FR_{23}: Calculate the axis track of the rotor-bearing system
- FR_{24}: Calculate the Poincare mapping of the rotor-bearing system

In order to satisfy these four FRs, four DPs can be selected as follows:

- DP_{21}: The vertical and horizontal displacement-time curves
- DP_{22}: The Fast Fourier transform
- DP_{23}: The vertical displacement-horizontal displacement curve
- DP_{24}: The vertical displacement-horizontal displacement point graph for every other period

The design equation can be written as:

$$\begin{Bmatrix} FR_{21} \\ FR_{22} \\ FR_{23} \\ FR_{24} \end{Bmatrix} = \begin{bmatrix} X & 0 & 0 & 0 \\ 0 & X & 0 & 0 \\ 0 & 0 & X & 0 \\ 0 & 0 & 0 & X \end{bmatrix} \begin{Bmatrix} DP_{21} \\ DP_{22} \\ DP_{23} \\ DP_{24} \end{Bmatrix} \tag{7}$$

The design matrix is a diagonal matrix, which indicates that this is an uncoupled design.

For DP_3, the critical speed and the threshold speed of the rotor-bearing system needs to be designed and the parameter regions where the system generates subharmonic resonances need to be identified by varying the characteristic parameters of the system. FR_3 can be decomposed as follows:

- FR_{31}: Design the critical speed of the rotor-bearing system
- FR_{32}: Design the threshold speed of the rotor-bearing system
- FR_{33}: Design the subharmonic resonance parameters of the rotor-bearing system

In order to meet these three FRs, three DPs can be chosen as follows:

- DP_{31}: The amplitude-speed curves of the system in the critical speed range
- DP_{32}: The frequency spectrum of the system
- DP_{33}: The amplitude-speed curves of the system at twice the critical speed range

The design equation can be written as:

$$\begin{Bmatrix} FR_{31} \\ FR_{32} \\ FR_{33} \end{Bmatrix} = \begin{bmatrix} X & 0 & 0 \\ 0 & X & 0 \\ 0 & 0 & X \end{bmatrix} \begin{Bmatrix} DP_{31} \\ DP_{32} \\ DP_{33} \end{Bmatrix} \tag{8}$$

The design matrix is a diagonal matrix, which illustrates that this is an uncoupled design.

Therefore, the second level design meets the independence axiom.

3.3. Decomposition of FRs and mapping of corresponding DPs at the third level

For DP_{11}, the calculation precision and speed both need to be improved when solving Reynolds equation, but there are some difficulties in simultaneously improving the precision and the speed. FR_{11} can be decomposed as follows:

- FR_{111}: Improve the calculation precision
- FR_{112}: Guarantee this precision and then improve the calculation speed

In order to meet these two FRs, two DPs can be chosen as follows:

- DP_{111}: Finite element method
- DP_{112}: The nonlinear oil film-force database based on the Poincare transformation [11]

The design equation can be written as:

$$\begin{Bmatrix} FR_{111} \\ FR_{112} \end{Bmatrix} = \begin{bmatrix} X & 0 \\ X & X \end{bmatrix} \begin{Bmatrix} DP_{111} \\ DP_{112} \end{Bmatrix} \tag{9}$$

The design matrix is a lower triangular matrix, which indicates that this is a decoupled design.

The rotor motion equation built by DP_{12} is a high-dimensional nonlinear kinetic equation with multiple degrees of freedom, which results in an extremely low solution efficiency. Therefore, dimension reduction of the high-dimensional nonlinear system must be obtained before solving the kinetic equation by numerical methods. FR_{12} can be decomposed as follows:

- FR_{121}: Reduce the dimensions of the high-dimensional nonlinear system
- FR_{122}: Solve the kinetic equation by numerical methods

In order to meet these two FRs, two DPs can be chosen as follows:

- DP_{121}: Fixed interface modal synthesis method
- DP_{122}: Runge-Kutta-Fehlberg method

The design equation can be written as:

$$\begin{Bmatrix} FR_{121} \\ FR_{122} \end{Bmatrix} = \begin{bmatrix} X & 0 \\ X & X \end{bmatrix} \begin{Bmatrix} DP_{121} \\ DP_{122} \end{Bmatrix} \tag{10}$$

The design matrix is a lower triangular matrix, which indicates that this is a decoupled design.

For DP_{31} and DP_{32}, the vertical and horizontal critical speed and the threshold speed of the rotor-bearing system need to be calculated for different levels of imbalance, because typically the nonlinear phenomenon is seen at

different critical speeds and threshold speeds of the rotor for different levels of rotor imbalance. FR_{31} and FR_{32} can be decomposed as follows:

- FR_{311}: Calculate the critical speed of the system under a low level of imbalance
- FR_{312}: Calculate the critical speed of the system under an allowable level of imbalance
- FR_{313}: Calculate the critical speed of the system under a high level of imbalance
- FR_{321}: Calculate the threshold speed of the system under a low level of imbalance
- FR_{322}: Calculate the threshold speed of the system under an allowable level of imbalance
- FR_{323}: Calculate the threshold speed of the system under a high level of imbalance

In order to satisfy these FRs, DPs can be chosen as follows:

- DP_{311}: The amplitude-speed curve of the system under a low level of imbalance
- DP_{312}: The amplitude-speed curve of the system under an allowable level of imbalance
- DP_{313}: The amplitude-speed curve of the system under a high level of imbalance
- DP_{321}: The frequency spectrum of the system under a low level of imbalance
- DP_{322}: The frequency spectrum of the system under an allowable level of imbalance
- DP_{323}: The frequency spectrum of the system under a high level of imbalance

The two design equations can be written as:

$$\begin{Bmatrix} FR_{311} \\ FR_{312} \\ FR_{313} \end{Bmatrix} = \begin{bmatrix} X & 0 & 0 \\ 0 & X & 0 \\ 0 & 0 & X \end{bmatrix} \begin{Bmatrix} DP_{311} \\ DP_{312} \\ DP_{313} \end{Bmatrix} \tag{11}$$

$$\begin{Bmatrix} FR_{321} \\ FR_{322} \\ FR_{323} \end{Bmatrix} = \begin{bmatrix} X & 0 & 0 \\ 0 & X & 0 \\ 0 & 0 & X \end{bmatrix} \begin{Bmatrix} DP_{321} \\ DP_{322} \\ DP_{323} \end{Bmatrix} \tag{12}$$

The two design matrices are both diagonal matrices, which indicates that they are uncoupled designs.

For DP_{33}, the speed range when subharmonic resonances occur in the rotor-bearing system and the impact of different system characteristic parameters such as imbalance, bearing types and lubricating oil viscosity on the subharmonic resonances of the system need to be considered. FR_{33} can be decomposed as follows:

- FR_{331}: Consider the impact of the rotor speed
- FR_{332}: Consider the impact of the rotor imbalance
- FR_{333}: Consider the impact of the bearing types
- FR_{334}: Consider the impact of the lubricating oil viscosity

In order to meet these four FRs, the rotor's amplitude at different speeds needs to be calculated under conditions of different system characteristic parameters. The four DPs can be chosen as follows:

- DP_{331}: The amplitudes of the system at different speeds
- DP_{332}: The amplitude-speed curves of the system under different levels of imbalance
- DP_{333}: The amplitude-speed curves of the system under different bearing type conditions
- DP_{334}: The amplitude-speed curves of the system under different lubricating oil viscosity conditions

The design equation can be written as:

$$\begin{Bmatrix} FR_{331} \\ FR_{332} \\ FR_{333} \\ FR_{334} \end{Bmatrix} = \begin{bmatrix} X & 0 & 0 & 0 \\ X & X & 0 & 0 \\ X & 0 & X & 0 \\ X & 0 & 0 & X \end{bmatrix} \begin{Bmatrix} DP_{331} \\ DP_{332} \\ DP_{333} \\ DP_{334} \end{Bmatrix} \tag{13}$$

The design matrix is a lower triangular matrix, which illustrates that this is a decoupled design.

Therefore, the third level design meets the independence axiom.

3.4. Decomposition of FRs and mapping of corresponding DPs at the fourth level

For DP_{322}, it is feasible to consider the impact of parameters such as the bearing ellipticity and the lubricating oil viscosity on the threshold speed of the rotor-bearing system under allowable levels of imbalance. The stability of the rotor-bearing system is very important in nonlinear rotor dynamic design, as it severely restricts the work efficiency and reliability of the power units. Therefore, measurements and schemes that improve the stability margin of the system should be considered before calculation. FR_{322} can be decomposed as follows:

- FR_{3221}: Consider the impact of the bearing ellipticity on the threshold speed
- FR_{3222}: Consider the impact of the lubricating oil viscosity on the threshold speed

In order to meet these two FRs, two DPs can be chosen as follows:

- DP_{3221}: The frequency spectrum of the system under different bearing ellipticity conditions
- DP_{3222}: The frequency spectrum of the system under different lubricating oil viscosity conditions

The design equation can be written as:

$$\begin{Bmatrix} FR_{3221} \\ FR_{3222} \end{Bmatrix} = \begin{bmatrix} X & 0 \\ 0 & X \end{bmatrix} \begin{Bmatrix} DP_{3221} \\ DP_{3222} \end{Bmatrix} \tag{14}$$

The design matrix is a diagonal matrix, which indicates that this is an uncoupled design.

For DP_{333}, two bearing types should be considered: circular journal bearings and elliptical journal bearings. FR_{333} can be decomposed as follows:

- FR_{3331}: Consider the impact of the circular journal bearings
- FR_{3332}: Consider the impact of the elliptical journal bearings

In order to meet these two FRs, two DPs can be chosen as follows:

- DP_{3331}: The amplitude-speed curves of the system under circular journal bearing conditions
- DP_{3332}: The amplitude-speed curves of the system under elliptical journal bearing conditions

The design equation can be written as:

$$\begin{Bmatrix} FR_{3331} \\ FR_{3332} \end{Bmatrix} = \begin{bmatrix} X & 0 \\ 0 & X \end{bmatrix} \begin{Bmatrix} DP_{3331} \\ DP_{3332} \end{Bmatrix} \tag{15}$$

The design matrix is a diagonal matrix, which illustrates that this is an uncoupled design.

Therefore, the fourth level design meets the independence axiom.

3.5. Global design matrix and design flowchart

The FRs and DPs of the supercritical rotor dynamic design based on axiomatic design theory have been decomposed to generate a level structure of the FRs and DPs by repeated iterations between the functional domain and the physical domain, as shown in Fig.4. The final decomposition result gives the twenty FRs and their corresponding DPs represented by the green frames. A 20×20 global design matrix is developed using the relationship between the FRs and DPs described by the design matrices at all levels, as shown in Table 1. The global design matrix is a lower triangular matrix, therefore, the supercritical rotor dynamic design is a decoupled design and meets the independence axiom.

Through the analysis of Fig.4 and Table 1, a dynamic design flowchart of the supercritical rotor-bearing system shown in Fig.5 can be obtained. Ⓢ is an AND node which means that there is an uncoupled design between modules without the need to consider the sequence in the design. © is a control node which means that there is a decoupled design between the modules that must be controlled in accordance with the sequence suggested by the design matrix during the design. Module M_i is defined as a single row of the design matrix, meaning that DP_i being input, FR_i can be determined. M_i can be expressed as:

$$M_i = \sum_{j=1}^{j=i} \frac{\partial FR_i}{\partial DP_j} \frac{DP_j}{DP_i} \tag{16}$$

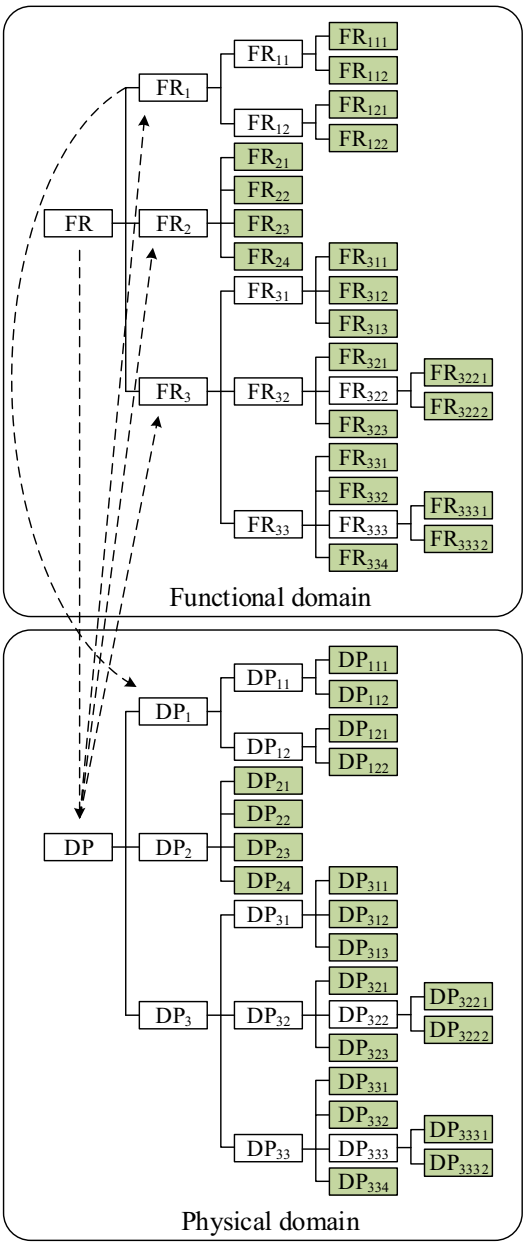

Fig. 4. The level structure of the FRs and DPs of the supercritical rotor dynamic design.

4. Design example and analysis

A single span flexible symmetric rotor-bearing system with a single disk is shown in Fig.6. The rotor parameters are shown in Table 2. The disk parameters are shown in Table 3. The bearing parameters are shown in Table 4. Under the guidance of the dynamic design flowchart for the supercritical rotor-bearing system, the rotor-bearing system is designed and analyzed. Although not described in detail in this example, Module M_1 is achieved using Fortran language.

Table 1. The global design matrix for supercritical rotor dynamics.

	DP_{111}	DP_{112}	DP_{121}	DP_{122}	DP_{21}	DP_{22}	DP_{23}	DP_{24}	DP_{311}	DP_{312}	DP_{313}	DP_{321}	DP_{3221}	DP_{3222}	DP_{323}	DP_{331}	DP_{332}	DP_{3331}	DP_{3332}	DP_{334}
FR_{111}	X	0	0	0	0	0	0	0	0	0	0	0	0	0	0	0	0	0	0	0
FR_{112}	X	X	0	0	0	0	0	0	0	0	0	0	0	0	0	0	0	0	0	0
FR_{121}	X	X	X	0	0	0	0	0	0	0	0	0	0	0	0	0	0	0	0	0
FR_{122}	X	X	X	X	0	0	0	0	0	0	0	0	0	0	0	0	0	0	0	0
FR_{21}	X	X	X	X	X	0	0	0	0	0	0	0	0	0	0	0	0	0	0	0
FR_{22}	X	X	X	X	0	X	0	0	0	0	0	0	0	0	0	0	0	0	0	0
FR_{23}	X	X	X	X	0	0	X	0	0	0	0	0	0	0	0	0	0	0	0	0
FR_{24}	X	X	X	X	0	0	0	X	0	0	0	0	0	0	0	0	0	0	0	0
FR_{311}	X	X	X	X	0	0	0	0	X	0	0	0	0	0	0	0	0	0	0	0
FR_{312}	X	X	X	X	0	0	0	0	0	X	0	0	0	0	0	0	0	0	0	0
FR_{313}	X	X	X	X	0	0	0	0	0	0	X	0	0	0	0	0	0	0	0	0
FR_{321}	X	X	X	X	0	X	0	0	0	0	0	X	0	0	0	0	0	0	0	0
FR_{3221}	X	X	X	X	0	X	0	0	0	0	0	0	X	0	0	0	0	0	0	0
FR_{3222}	X	X	X	X	0	X	0	0	0	0	0	0	0	X	0	0	0	0	0	0
FR_{323}	X	X	X	X	0	X	0	0	0	0	0	0	0	0	X	0	0	0	0	0
FR_{331}	X	X	X	X	0	0	0	0	0	0	0	0	0	0	0	X	0	0	0	0
FR_{332}	X	X	X	X	0	0	0	0	0	0	0	0	0	0	0	X	X	0	0	0
FR_{3331}	X	X	X	X	0	0	0	0	0	0	0	0	0	0	0	X	0	X	0	0
FR_{3332}	X	X	X	X	0	0	0	0	0	0	0	0	0	0	0	X	0	0	X	0
FR_{334}	X	X	X	X	0	0	0	0	0	0	0	0	0	0	0	X	0	0	0	X

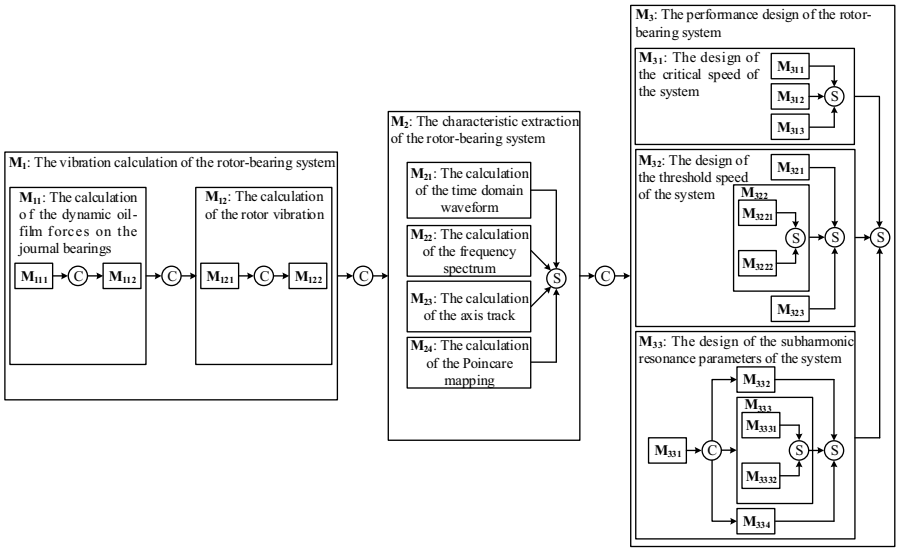

Fig. 5. The dynamic design flowchart of the supercritical rotor-bearing system.

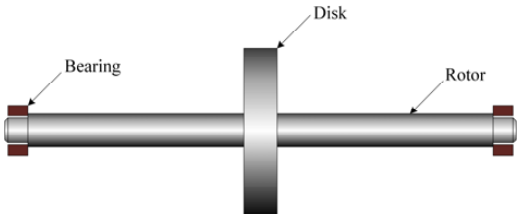

Fig. 6. The rotor-bearing system diagram.

Table 2. The rotor parameters.

Length (m)	Diameter (m)	Density ($kg \cdot m^{-3}$)	Elasticity modulus (Pa)
2.8	0.2	7.8×10^{3}	2.0×10^{11}

Table 3. The disk parameters.

Mass (kg)	Diameter moment of inertia ($kg \cdot m^2$)	Polar moment of inertia ($kg \cdot m^2$)	Mass eccentricity (μm)	imbalance ($g \cdot mm$)
1176.21	80.37	152.91	25	29405.25

Table 4. The bearing parameters.

Diameter (*m*)	Length (*m*)	Radial clearance (*μm*)	Tile wrap angle (°)	Ellipticity	Lubricating oil viscosity (*Pa·s*)
0.15	0.12	225	150	0.4	0.005

4.1. Realization of Module M_2

The characteristic extraction graph of the left axle journal vibration at a speed of 3000rpm is shown in Fig.7. The rotor maintains a synchronous periodic motion around the moment. The vibration frequency is only a working frequency. The axis track appears as an ellipse, and only a fixed point is shown in the Poincare mapping diagram. The characteristic extraction graph of the left axle journal vibration at a speed of 3500rpm is shown in Fig.8. The rotor maintains a quasiperiodic motion around the moment. A low frequency component is seen in the frequency spectrogram as well as the working frequency. The axis track forms a ribbon pattern with a certain width, and a closed point ring is shown in the Poincare mapping diagram.

4.2. Realization of Module M_3

The implementation result of Module M_{31} is shown in Fig.9. It can be seen from this figure that the first critical speed of the system is slightly different for different levels of disk imbalance. Appropriate increases in the disk imbalance can raise the horizontal critical speed and lower the vertical critical speed.

The implementation results of Module M_{32} are shown in Table 5. The instability refers to the variation from a synchronous periodic motion to a quasiperiodic motion, but not including the quasiperiodic motion at the subharmonic resonance speed. Table 5 shows that an appropriate increase of the imbalance and ellipticity, and an appropriate reduction of the lubricating oil viscosity, can improve the stability of the system.

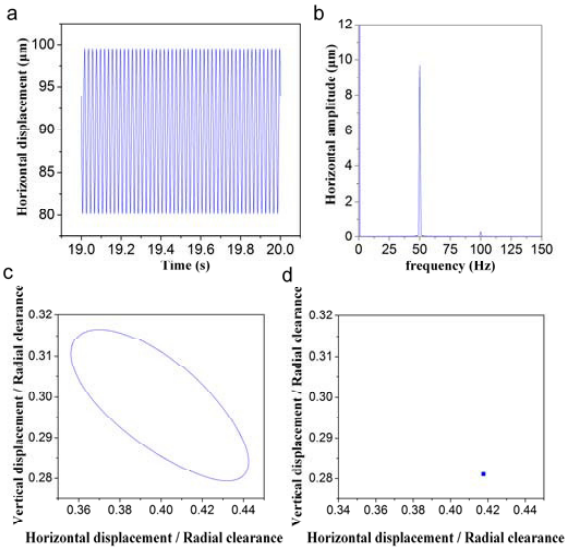

Fig. 7. The characteristic extraction graph of the left axle journal vibration at a speed of 3000rpm: (a) the time domain waveform; (b) the frequency spectrum; (c) the axis track; (d) the Poincare mapping.

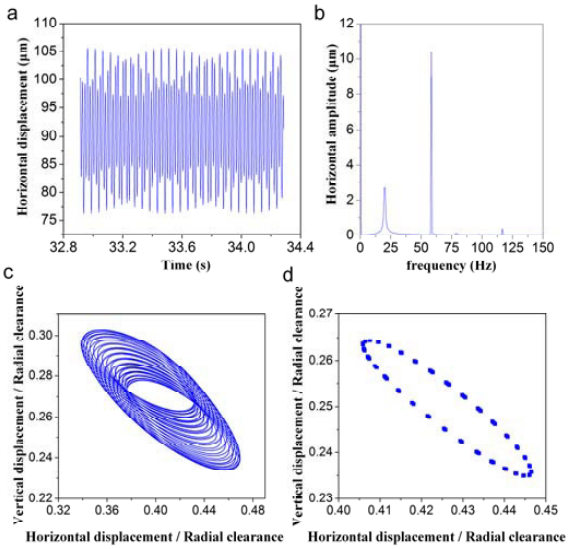

Fig. 8. The characteristic extraction graph of the left axle journal vibration at a speed of 3500rpm: (a) the time domain waveform; (b) the frequency spectrum; (c) the axis track; (d) the Poincare mapping.

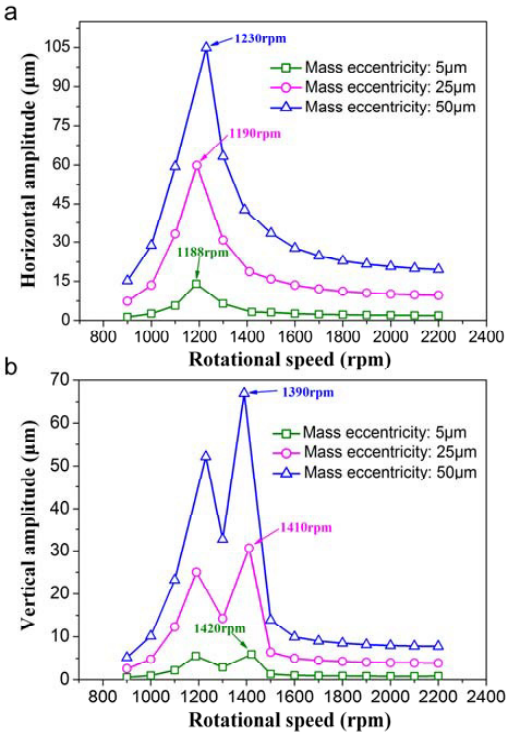

Fig. 9. The amplitude-speed curve of the left axle journal vibration under different levels of imbalance: (a) the horizontal amplitude-speed curve; (b) the vertical amplitude-speed curve.

Table 5. The threshold speed of the system under conditions of different ellipticity, lubricating oil viscosity and mass eccentricity.

Ellipticity	Lubricating oil viscosity (*Pa·s*)	Mass eccentricity (*μm*)	Threshold speed (*rpm*)
0.4	0.005	25	3410
0.5	0.005	25	4280
0.6	0.005	25	4830
0.4	0.002	25	5200
0.4	0.01	25	2940
0.4	0.005	5	3180
0.4	0.005	75	3440

The implementation results of Module M_{332} are shown in Fig.10. While the disk imbalance increases to a certain extent, the rotor vibration peak also appears at approximately double the first critical speed, which means that one half-subharmonic resonance of the system occurs. In order to analyze the dynamic behavior of the system at a speed of one half-subharmonic resonance, the axis track chart and the Poincare mapping diagram of the system at a speed of 2590rpm with a mass eccentricity of 70μm are given, as shown in Fig.11. The rotor maintains a quasiperiodic motion around the moment, but returns to a synchronous periodic orbit above the half-subharmonic resonance speed.

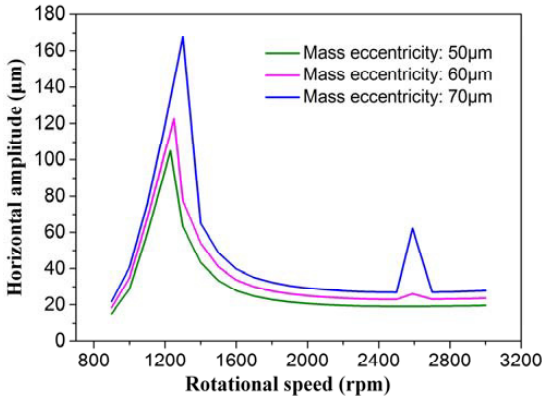

Fig. 10. The amplitude-speed curve of the left axle journal vibration under different levels of imbalance.

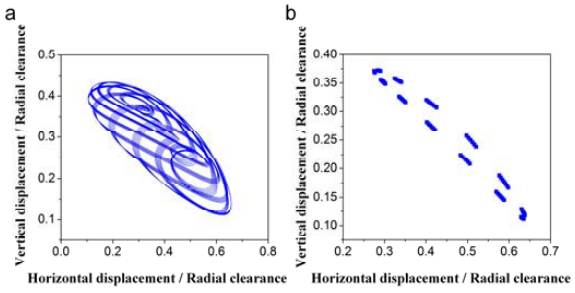

Fig. 11. The axis track chart and the Poincare mapping diagram of the system at a speed of 2590rpm with a mass eccentricity of 70μm: (a) the axis track; (b) the Poincare mapping.

The implementation results of Module M_{333} and Module M_{334} are shown in Fig.12. Under circular journal bearing conditions, the system can more easily generate one half-subharmonic resonance than under elliptical journal bearing conditions. The system is less likely to generate one half-subharmonic resonance under higher oil viscosity conditions.

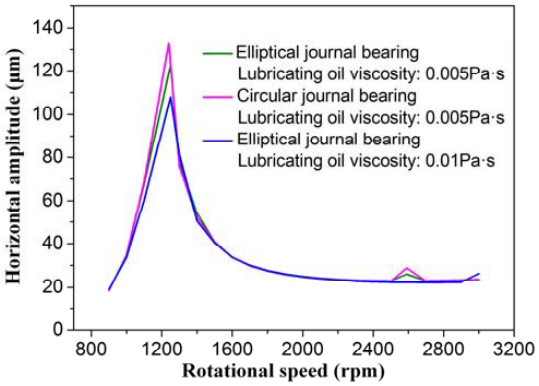

Fig. 12. The amplitude-speed curve of the left axle journal vibration under conditions of different bearing types and lubricating oil viscosity (mass eccentricity: 60μm).

5. Results and discussion

By analyzing the calculation results of the design example, it can be seen that a single span flexible symmetric rotor-bearing system with a single disk has its first horizontal critical speed at 1190 rpm, its first vertical critical speed at 1410 rpm and a threshold speed of 3410 rpm. The rotor maintains a synchronous periodic motion when it is operating below a speed of 3410 rpm and maintains a quasiperiodic motion when it is operating within a certain range beyond a speed of 3410 rpm. In comparison with circular journal bearings, choosing elliptical journal bearings in the design can improve the stability of the system and less easily cause one half-subharmonic resonance of the system. A higher level of rotor imbalance in the design can raise the horizontal critical speed of the system, lower the vertical critical speed of the system and improve the stability of the system, but it can also increase the rotor's vibration amplitude and even cause one half-subharmonic resonance of the system. A lower lubricating oil viscosity in the design can improve the stability of the system, but can also cause one half-subharmonic resonance. Therefore, taking various factors into consideration, designers should choose appropriate characteristic parameters to realize a supercritical rotor dynamic design according to specific design requirements.

When nonlinear effects are stronger in rotor-bearing systems, there are obvious differences in the design results for the critical speed and threshold speed between rotor dynamic design methods that consider nonlinear deep knowledge and designs based only on linear theory. The first horizontal critical speed and threshold speed of the rotor-bearing system with a disk mass eccentricity of 75μm based on linear and nonlinear theories are given in Table 6. It can be seen that when nonlinear deep knowledge is considered, the first

horizontal critical speed improves by 15.6 percent and the threshold speed improves by 8.9 percent. Therefore, the nonlinear factors of rotor-bearing systems cannot be ignored in the supercritical rotor dynamic design. After adopting an axiomatic design method which integrates nonlinear deep knowledge, the critical speed and threshold speed that are calculated are closer to actual working conditions, thus optimizing the design results.

Table 6. The first horizontal critical speed and threshold speed of the system with a disk mass eccentricity of 75μm based on linear and nonlinear theories.

	Horizontal critical speed (*rpm*)	Threshold speed (*rpm*)
Linear theory	1185	3160
Nonlinear theory	1370	3440
Improved degree (%)	15.6	8.9

6. Conclusions

(1) In order to introduce nonlinear theory of rotor-bearing systems into rotor dynamic design and integrate the nonlinear deep knowledge research, an axiomatic design method for supercritical rotor dynamics has been adopted. A four-level decomposition of FRs and mapping of corresponding DPs have been achieved. A global design matrix for supercritical rotor dynamics has then been developed. A dynamic design flowchart of the rotor-bearing system has finally been obtained.

(2) Under the guidance of the design flowchart, a single span flexible symmetric rotor-bearing system with a single disk has been dynamically designed and analyzed. The feasibility and validity of axiomatic design theory for supercritical rotor dynamic design has been validated. The design results that consider nonlinear deep knowledge have been found to be superior to those based only on linear theory.

(3) Appropriate increases in the rotor imbalance can raise the horizontal critical speed of the rotor-bearing system and lower the vertical critical speed of the system. Appropriate increases in the imbalance and ellipticity, and reductions in the lubricating oil viscosity can improve the stability of the system. The rotor-bearing system is more likely to generate one half-subharmonic resonance under circumstances of a larger imbalance, lower lubricating oil viscosity and circular journal bearings. These various factors need to be considered by designers in order to select appropriate parameters to achieve a supercritical rotor dynamic design according to specific design requirements.

Acknowledgements

Financial support provided by the subproject of National Key Basic Research Program of China (2015CB057303-2) is gratefully acknowledged.

References

[1] Huang W, Wu X, Jiao Y, Xia S, Chen Z. Review of Nonlinear Rotor Dynamics. Journal of Vibration Engineering 2000;13:4, p. 497-509.
[2] Wu X, Lin B, Liu F, Han X. Review of Nonlinear Rotor-Bearing Dynamics System. Applied Mechanics and Materials 2010;37-38, p. 1130-1137.
[3] Suh NP. Axiomatic design: Advances and applications. New York: Oxford University Press; 2001.
[4] Xie Y, Yuan X, Xu H, Dong G, et al. Axiomatic design—Advances and applications. Beijing: China Machine Press; 2004.
[5] Babic B. Axiomatic design of flexible manufacturing systems. International Journal of Production Research 1999;37:5, p. 1159-1173.
[6] Durmusoglu MB, Satoglu SI. Axiomatic design of hybrid manufacturing systems in erraticdemand conditions. International Journal of Production Research 2011;49:17, p. 5231-5261.
[7] Li JW, Chen XB, Zhang WJ. Axiomatic-Design-Theory-Based Approach to Modeling Linear High Order System Dynamics. IEEE/ASME Transactions on Mechatronics 2011;16:2, p. 341-350.
[8] Bae TS, Lee KH. Structural Design of a Main Starting Valve Based on the First Axiom. International Journal of Precision Engineering and Manufacturing 2012;13:5, p. 685-691.
[9] Xi W, Xu J, Zhang H, Lu Z, Yuan X. Investigation on Influences of Labyrinth Seal on Stability of High-parameter Rotor System and Application of Axiomatic Design Method. Proceedings of the CSEE 2013;33:5, p. 102-111.
[10] Zhang G, Zhao W, Yan X, Wei J, Chen Y. Axiomatic Design Method for the Rotor Dynamics of the Multi-sourceInformation Coupled High-speed Turbopump. Journal of Mechanical Engineering 2015;51:5, p. 47-55.
[11] Meng Z, Xu H, Zhu J. A Database Method of Nonlinear Oil Film Force Based on Poincare Transformation. Tribology 2001;21:3, p. 223-227.